

PREPARED FOR SUBMISSION TO JHEP

Complex Langevin Dynamics for chiral Random Matrix Theory

A. Mollgaard^a K. Splittorff^a

^aDiscovery Centre, Niels Bohr Institute, University of Copenhagen, Blegdamsvej 17, 2100 Copenhagen Ø, Denmark

ABSTRACT: We apply complex Langevin dynamics to chiral random matrix theory at nonzero chemical potential. At large quark mass the simulations agree with the analytical results while incorrect convergence is found for small quark masses. The region of quark masses for which the complex Langevin dynamics converges incorrectly is identified as the region where the fermion determinant frequently traces out a path surrounding the origin of the complex plane during the Langevin flow. This links the incorrect convergence to an ambiguity in the Langevin force due to the presence of the logarithm of the fermion determinant in the action.

1 Introduction

Understanding the phase diagram of QCD in the chemical potential, μ , and temperature, T , plane is one of the greatest challenges of high energy physics today. At $\mu = 0$, QCD may be treated on the lattice, but for $\mu \neq 0$ the fermion determinant turns complex

$$\det \equiv \det (i\gamma_\nu D_\nu + \mu\gamma_0 + m) \in \mathbb{C}, \quad (1.1)$$

such that a reweighting is needed to apply importance sampling. The numerical computations grow exponentially harder as the volume is increased, and this complication has been named the “the sign problem” (see [1–3] for reviews).

An interesting method for generating field configurations according to the probabilistic weight at $\mu = 0$ is that of Langevin dynamics [4]. Unlike other approaches, Langevin dynamics may naturally be generalized to the case of complex weights, but tools to check the results of such simulations have not been available until recently [5–7]. Not only have we gained improved understanding; complex Langevin dynamics has also been applied to solve sign problems in a number of physical models such as the relativistic Bose gas [8–10] and a one-dimensional version of QCD [11]. Moreover, the technique of gauge cooling has very recently been introduced to obtain well behaved dynamics in the case of QCD in the heavy quark mass limit [13, 14] as well as in full QCD [15]. In this paper we apply complex Langevin dynamics to chiral random matrix theory at nonzero chemical potential [16, 17]. Just as in QCD the sign problem of chiral random matrix theory comes in through the presence of a complex valued fermion determinant. The advantage of the random matrix theory is that exact analytic solutions are known and allow for a direct test of the complex Langevin simulation.

Our main objective with the simulation of chiral random matrix theory is to understand to which degree complex Langevin dynamics (CLD) is able to deal with a complex valued fermion determinant. The standard approach of complex Langevin is first to exponentiate the fermion determinant,

$$\det(M) e^{-S_g} = e^{-S_g + \log(\det(M))}, \quad (1.2)$$

and subsequently obtain the Langevin drift term by taking the derivative of the action, $S \equiv S_g - \log(\det(M))$, with respect to the relevant fields. At this point, however, one is faced with an ambiguity because the logarithm is a multivalued function. On one hand one could argue that the derivative of the logarithm in the complex plane is well defined on the infinite Riemann sheet and simply extend the standard derivative, $d \log f(x)/dx = f'(x)/f(x)$, into the full complex plane. On the other hand one could

choose to work with principal part of the logarithm which is single-valued, but has a branch cut from the origin along the negative real axis. The imaginary part is discontinuous across this cut and the derivative is therefore not straightforward to implement in the Langevin force. However, since the imaginary part of the logarithm is exactly what allows $\exp(\log(\det(M)))$ to change sign when the determinant moves from positive to negative values on the real axis it is natural to expect that the influence of the cut on the Langevin flow is essential.

In the Langevin simulation of the chiral random matrix theory we will follow [13–15] and make use of the standard form of the derivative of the logarithm. We observe that while the Langevin dynamics reproduce the analytical results at large values of the quark mass, failed convergence is found for small masses. We identify the range of quark masses for which the complex Langevin dynamics converges to incorrect values as the region where the determinant frequently traces out a path surrounding the origin of the complex plane. The results of the Langevin dynamics in this region are similar in nature to the results obtained in the phase quenched chiral random matrix theory. This suggests that the cut is relevant for the Langevin dynamics and should not be ignored in the flow equations.

As the derivative of the logarithm is unique on the full principal branch the ambiguity of the Langevin flow is only relevant when the determinant frequently circles the origin. We use this to predict regions of successful and failed convergence in two previously studied $U(1)$ models [11, 18]. It is likely also to explain the crossover from successful to failed complex Langevin dynamics in other models with a logarithm in the action such as the Thirring model [19].

The outline of the article is the following: in section 2 we give a more detailed introduction to the Langevin equation, and in section 3 we take a closer look at the logarithm. Section 4 is devoted to the application of complex Langevin dynamics to chiral random matrix theory, and the two $U(1)$ models are discussed in section 5. Finally in section 6 we summarize the results and offer a look ahead. In the appendix we revisit the $U(1)$ model of [20].

2 The Langevin equation

The real Langevin equation provides a method for generating ensembles of field configurations according to the positive weight function at $\mu = 0$. For simplicity let us first

consider a single real variable, x , with a partition function

$$Z = \int e^{-S(x)} dx, \quad (2.1)$$

and a positive weight

$$e^{-S(x)} \in \mathbb{R}_+. \quad (2.2)$$

The real Langevin equation then takes the form

$$x(t + dt) = x(t) - \partial_x S(x(t)) \cdot dt + dW, \quad (2.3)$$

where dW is a stochastic variable of zero mean $\langle dW \rangle = 0$ and variance $\langle dW^2 \rangle = 2dt$. Analytic mean values

$$\langle O(x) \rangle = \frac{\int dx O(x) e^{-S(x)}}{Z} \quad (2.4)$$

may be calculated numerically by updating the variable according to (2.3) and calculating the observable value with each step; the mean value of such measurements approaches the analytic result as $t \rightarrow \infty$ [21].

As proposed by Parisi [22] and Klauder [23] we may generalize the Langevin equation to complex weights using the drift

$$\left. \frac{dS(x)}{dx} \right|_{x \rightarrow x+iy}. \quad (2.5)$$

The variable is then pushed off the real axis and into the complex plane, $x \rightarrow z = x+iy$, where Langevin measurements may be performed as in the case of real and positive weights. The proof relating Langevin dynamics to the path integral no longer applies though (see [14]), and simulations only converge correctly some of the time. In order to have a well defined drift term, (2.5), in the whole complex plane, we need the action to be entire, such that the Langevin equation may be written uniquely as

$$z(t + dt) = z(t) - \partial_z S(z(t)) \cdot dt + dW. \quad (2.6)$$

Two criteria for correct convergence have been given for such entire actions in [5–7].

The Langevin equation trivially generalizes to theories with more degrees of freedom, such as QCD on the lattice. The Euclidian partition function is given as an integral over the link variables U and has the structure

$$Z = \int \mathcal{D}U \det M \cdot e^{-S_g}, \quad (2.7)$$

where S_g is the Yang-Mills term and $\det M$ is the fermion determinant (see eg [24]). For $\mu \neq 0$ the fermion determinant turns complex, such that for example a reweighting must be performed or the complex Langevin equation must be applied. Reweighting is exponentially hard in the volume [25] because of the sign problem, so we turn to complex Langevin dynamics (CLD). In order to go beyond the quenched approximation we include the fermion determinant into the action

$$S = S_g - \log(\det M), \quad (2.8)$$

which determines the Langevin flow through (2.6). As we now discuss, such a logarithmic term in the action leads to an ambiguity in the complex Langevin dynamics.

3 The logarithm

The logarithm is a multivalued function with output

$$\log(z) = \text{Log}(z) + i2\pi \cdot n, \quad (3.1)$$

where $\text{Log}(z)$ is the principal part of the logarithm and $n \in \mathbb{Z}$. Any definition of the logarithm compatible with (3.1) yields the same weight in the original path integral, but the Langevin flow is determined from the action alone, so here it matters what definition is chosen. If we accept the use of a multivalued logarithm, then the derivative of the logarithm may be written as

$$\partial_z \log(z) = 1/z. \quad (3.2)$$

If we require a single valued logarithm and work with the principal part of the logarithm, then the derivative on the branch is still

$$\partial_z \text{Log}(z) = 1/z, \quad z \in \mathbb{C}/\mathbb{R}_-. \quad (3.3)$$

In addition, however, there will be a cut from the origin out to infinity, where the derivative is singular, see eg. [26] for a discussion.

In the next section we will adopt the first option where the cut is ignored, and demonstrate that simulations of chiral random matrix theory yield failed measurements, when the phase of the determinant, $\det M$, frequently circles the full range $[-\pi, \pi]$ during the Langevin simulation.

4 chiral Random Matrix Theory

Instead of approaching QCD head on we study chiral random matrix theory [27–29] with nonzero chemical potential, which has a similar structure with a fermion determinant in the measure, but at the same time is much simpler and possible to solve analytically. Chiral random matrix theory has already provided several deep insights into QCD at nonzero chemical potential: it has explained the failure of the quenched approximation [30], it has uncovered the OSV relation [31] which replaces the Banks-Casher relation [32] at nonzero chemical potential and it has revealed the surprising phase structure of QCD with bosonic quarks at nonzero chemical potential [33]. The reason why the far simpler random matrix theory can give direct insights into QCD is that the quark mass dependence of the chiral condensate and baryon density are uniquely determined by the flavor symmetries in the microscopic limit. Since QCD and chiral random matrix theory have the exact same flavor symmetries, we can use the analytic tools of chiral random matrix theory to derive the universal predictions for QCD.

The partition function reads

$$Z_N^{N_f}(m) = \int d\Phi d\Psi \det^{N_f} (D(\mu) + m) \exp \left(-N \cdot \text{Tr}[\Psi^\dagger \Psi + \Phi^\dagger \Phi] \right), \quad (4.1)$$

where

$$D(\mu) + m = \begin{pmatrix} m & i \cosh(\mu)\Phi + \sinh(\mu)\Psi \\ i \cosh(\mu)\Phi^\dagger + \sinh(\mu)\Psi^\dagger & m \end{pmatrix}. \quad (4.2)$$

The degrees of freedom, Ψ and Φ , are general complex $N \times N$ matrices, so $\Phi_{ij} = a_{ij} + ib_{ij}$, $\Psi_{ij} = \alpha_{ij} + i\beta_{ij}$ and $d\Phi d\Psi = da db d\alpha d\beta$. This chiral random matrix theory was introduced in [16], but uses the redefined parameters of [17]. Notice that

$$\det^*(D(\mu) + m) = \det(D(-\mu^*) + m) \quad (4.3)$$

just as in QCD. In the microscopic limit $N \rightarrow \infty$ with $\tilde{m} = Nm$ and $\tilde{\mu} = \sqrt{N}\mu$ kept constant, the matrix model may be shown to be equivalent to the ϵ -regime of chiral perturbation theory [16, 35–37].

4.1 Analytical results

We will consider the theory with two mass degenerate flavors, $N_f = 2$, and perform measurements of the mass dependent chiral condensate

$$\frac{1}{N} \langle \bar{\eta} \eta \rangle = \frac{1}{N} \partial_m \log(Z), \quad (4.4)$$

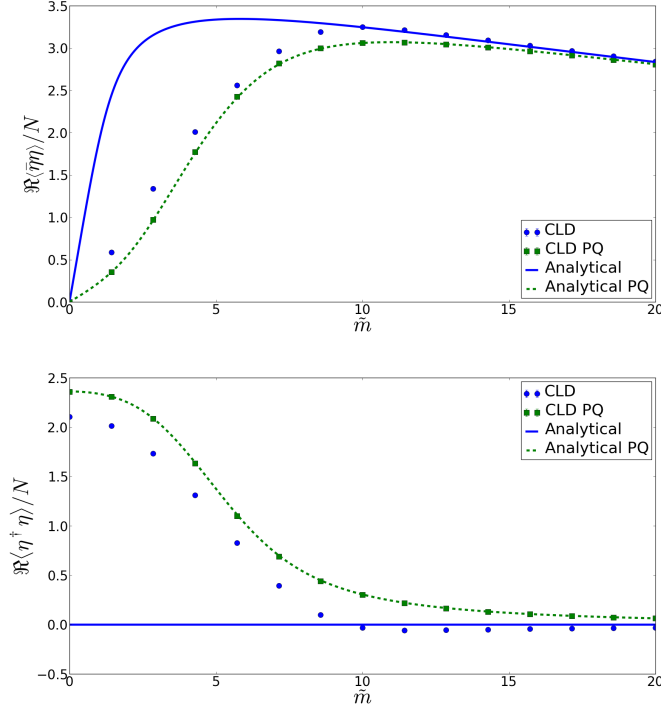


Figure 1. CLE measurement of the chiral condensate (top) and the baryon number density (bottom) for $t = 50$, $dt = 10^{-4}$, $N = 30$, $N_f = 2$, $\tilde{\mu} = 2$ and a range of masses. The circular blue dots represent a CLD simulation of the chiral random matrix theory in (4.1) and the blue line is the analytical result. We find correct convergence for large masses, but failed convergence for small masses. The phase quenched theory represented by the green squares and line, is simulated correctly in the full mass range. Error bars based on statistics from 3 different simulations are present, but too small to see.

and the baryon number density

$$\frac{1}{N} \langle \eta^\dagger \eta \rangle = \frac{1}{N} \partial_\mu \log(Z), \quad (4.5)$$

where $\bar{\eta}$ and η represent the quark fields. It may be shown [17] that the baryon number density vanishes

$$\frac{1}{N} \langle \eta^\dagger \eta \rangle_{\text{analytical}} = 0, \quad (4.6)$$

while the chiral condensate may be found from the closed form of the partition function in [16]

$$\frac{1}{N} \langle \bar{\eta} \eta \rangle_{\text{analytical}} = \frac{2m [L_N^0(x) L_{N-1}^2(x) - L_{N+1}^0(x) L_{N-2}^2(x)]}{L_N^0(x) L_N^1(x) - L_{N+1}^0(x) L_{N-1}^1(x)}, \quad (4.7)$$

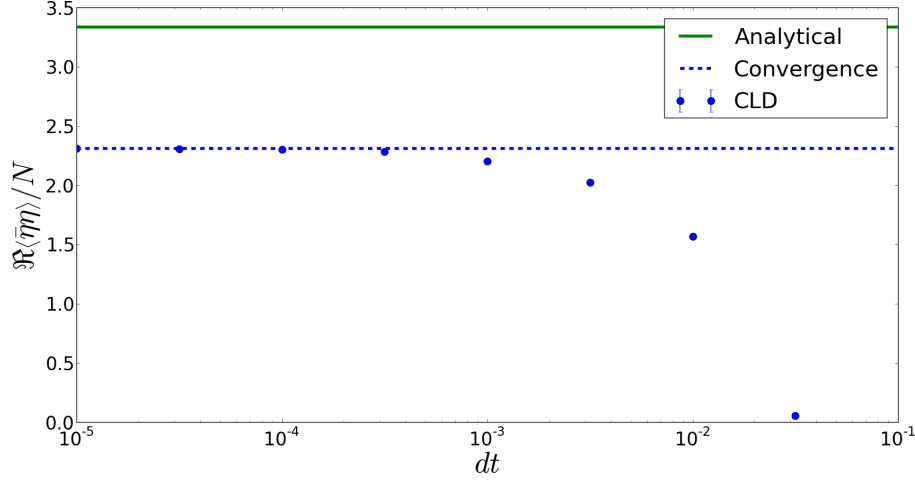


Figure 2. A plot of the chiral condensate as a function of dt for $t = 50$, $N = 30$, $N_f = 2$, $\tilde{\mu} = 2$ and $\tilde{m} = 5$. We find that the simulation settles around $dt = 10^{-4}$, but not to the true analytically derived value given by the green line.

with L_j^k being the generalized Laguerre polynomials and $x \equiv -Nm^2$. (Note that the μ -independence of the partition function in chiral random matrix theory corresponds to the μ -independence of chiral perturbation theory. The measure in the chiral random matrix theory is of course strongly μ -dependent, cf. (4.1).)

For comparison, we will also simulate the phase quenched theory, in which $\det^2(D(\mu) + m)$ is replaced by $|\det(D(\mu) + m)|^2$. The phase quenched chiral random matrix theory has been solved analytically in [35]. The chiral condensate is given as

$$\frac{1}{N} \langle \bar{\eta}\eta \rangle_{analytical}^{PQ} = 4m \frac{\sum_{j=0}^N \cosh(2\mu)^{-2j} L_j^0(x) L_{j-1}^1(x)}{\sum_{j=0}^N \cosh(2\mu)^{-2j} L_j^0(x)^2}, \quad (4.8)$$

while the baryon number density is

$$\frac{1}{N} \langle \eta^\dagger \eta \rangle_{analytical}^{PQ} = \frac{4 \tanh(2\mu)}{N} \left(\frac{\sum_{j=0}^N (N-j) \cdot \cosh(2\mu)^{-2j} L_j^0(x)^2}{\sum_{j=0}^N \cosh(2\mu)^{-2j} L_j^0(x)^2} \right). \quad (4.9)$$

Since the phase quenched theory can be simulated with real Langevin dynamics it serves as a partial check of the numerics.

4.2 Langevin dynamics

In order to optimize the simulation we reduce the dimensionality of the argument of the determinant

$$\det(D(\mu) + m) = \det \begin{pmatrix} m & X \\ Y & m \end{pmatrix} = \det(m^2 - XY), \quad (4.10)$$

where

$$X \equiv i \cosh(\mu) \Phi + \sinh(\mu) \Psi \quad (4.11)$$

and

$$Y \equiv i \cosh(\mu) \Phi^\dagger + \sinh(\mu) \Psi^\dagger. \quad (4.12)$$

Exponentiating the fermion determinant

$$Z_N^{N_f}(m) = \int d\Phi d\Psi \exp(N_f \cdot \text{Tr}[\log(m^2 - XY)] - N \cdot \text{Tr}[\Psi^\dagger \Psi + \Phi^\dagger \Phi]), \quad (4.13)$$

we obtain the action

$$S = N \cdot \text{Tr}[\Psi^\dagger \Psi + \Phi^\dagger \Phi] - N_f \cdot \text{Tr}[\log(m^2 - XY)]. \quad (4.14)$$

To derive the drift terms for $a_{ij}, b_{ij}, \alpha_{ij}, \beta_{ij}$ we write out the action in terms of these. The Gaussian part reads

$$\begin{aligned} \text{Tr}[\Psi^\dagger \Psi + \Phi^\dagger \Phi] &= \text{Tr}[(\Psi^\dagger)_{ij} \Psi_{jk} + (\Phi^\dagger)_{ij} \Phi_{jk}] \\ &= \Psi_{ji}^* \Psi_{ji} + \Phi_{ji}^* \Phi_{ji} \\ &= (\alpha_{ji} - i\beta_{ji})(\alpha_{ji} + i\beta_{ji}) + (a_{ji} - ib_{ji})(a_{ji} + ib_{ji}) \\ &= \alpha_{ji}^2 + \beta_{ji}^2 + a_{ji}^2 + b_{ji}^2, \end{aligned} \quad (4.15)$$

while the non diagonal terms of the determinant take the form

$$X_{ij} = i \cosh(\mu) (a_{ij} + ib_{ij}) + \sinh(\mu) (\alpha_{ij} + i\beta_{ij}) \quad (4.16)$$

and

$$\begin{aligned} Y_{ij} &= i \cosh(\mu) ((a + ib)^\dagger)_{ij} + \sinh(\mu) ((\alpha + i\beta)^\dagger)_{ij} \\ &= i \cosh(\mu) (a_{ji} - ib_{ji}) + \sinh(\mu) (\alpha_{ji} - i\beta_{ji}). \end{aligned} \quad (4.17)$$

We introduce the notation $G \equiv (m^2 - XY)^{-1}$ and calculate the drift term for a_{mn} (ignoring the cut)

$$\begin{aligned}
-\frac{\partial S}{\partial a_{mn}} &= -2Na_{mn} - N_f \cdot \text{Tr} \left[\left((m^2 - XY)^{-1} \right)_{li} \partial_{a_{mn}} (X_{ij} Y_{jk}) \right] \\
&= -2Na_{mn} - N_f \cdot \text{Tr} [G_{li} (i \cosh(\mu) \delta_{mi} \delta_{nj} Y_{jk} + i \cosh(\mu) X_{ij} \delta_{mk} \delta_{nj})] \\
&= -2Na_{mn} - N_f i \cosh(\mu) \cdot [G_{ki} (\delta_{mi} \delta_{nj} Y_{jk} + X_{ij} \delta_{mk} \delta_{nj})] \\
&= -2Na_{mn} - N_f i \cosh(\mu) \cdot [G_{km} Y_{nk} + G_{mi} X_{in}] \\
&= -2Na_{mn} - N_f i \cosh(\mu) \cdot \left[\left((YG)^\top \right)_{mn} + (GX)_{mn} \right] \\
&= -2Na_{mn} - iN_f \cosh(\mu) [R_{mn} + T_{mn}], \tag{4.18}
\end{aligned}$$

where we have defined

$$R_{mn} = \left((YG)^\top \right)_{mn} \tag{4.19}$$

and

$$T_{mn} = (GX)_{mn}. \tag{4.20}$$

The derivation of the other drift terms follow the same logic

$$\begin{aligned}
-\frac{\partial S}{\partial b_{mn}} &= -2Nb_{mn} + N_f \cosh(\mu) \cdot [R_{mn} - T_{mn}] \\
-\frac{\partial S}{\partial \alpha_{mn}} &= -2N\alpha_{mn} - N_f \sinh(\mu) \cdot [R_{mn} + T_{mn}] \\
-\frac{\partial S}{\partial \beta_{mn}} &= -2N\beta_{mn} - iN_f \sinh(\mu) \cdot [R_{mn} - T_{mn}]. \tag{4.21}
\end{aligned}$$

Turning to the Langevin simulation we count $2 \cdot 2 \cdot N^2$ real degrees of freedom to be complexified

$$a_{ij}, b_{ij}, \alpha_{ij}, \beta_{ij} \in \mathbb{R} \rightarrow a_{ij}, b_{ij}, \alpha_{ij}, \beta_{ij} \in \mathbb{C}, \tag{4.22}$$

such that we effectively need to update $8N^2$ degrees of freedom with each time step. Fast matrix manipulations may now be applied when updating the variables according to the complex Langevin equation

$$u_{ij}(t + \Delta t) = u_{ij}(t) - \frac{\partial S}{\partial u_{ij}} \cdot \Delta t + dW_{ij}, \tag{4.23}$$

where dW_{ij} is a Gaussian noise matrix

$$\langle dW_{ij} \rangle = 0, \quad \langle dW_{ij}(t) dW_{kl}(t') \rangle = 2dt \cdot \delta(t - t') \delta_{ik} \delta_{jl}, \tag{4.24}$$

and u_{ij} is representing any of $a_{ij}, b_{ij}, \alpha_{ij}, \beta_{ij}$.

The chiral condensate is obtained by differentiating the partition function (4.13) with respect to the mass

$$\begin{aligned}\frac{\bar{\eta}\eta}{N} &= \frac{N_f}{N} \partial_m (\text{Tr} [\log (m^2 - XY)]) \\ &= \frac{2mN_f}{N} \cdot \text{Tr} [(m^2 - XY)^{-1}].\end{aligned}\quad (4.25)$$

Differentiating with respect to the chemical potential gives the baryon number density

$$\begin{aligned}\frac{\eta^\dagger \eta}{N} &= \frac{N_f}{N} \partial_\mu (\text{Tr} [\log (m^2 - XY)]) \\ &= \frac{N_f}{N} \left(\text{Tr} [(m^2 - XY)^{-1} \partial_\mu (m^2 - XY)] \right) \\ &= \frac{N_f}{N} \left(\text{Tr} [(m^2 - XY)^{-1} (- (\partial_\mu X) Y - X (\partial_\mu Y))] \right).\end{aligned}\quad (4.26)$$

To obtain the dynamics of the phase quenched theory, we use the relation in equation (4.3) to write the absolute value as

$$\begin{aligned}|\det(D(\mu) + m)|^{N_f} &= [\det(D(\mu) + m) \det^*(D(\mu) + m)]^{N_f/2} \\ &= \det^{N_f/2}(D(\mu) + m) \det^{N_f/2}(D(-\mu) + m).\end{aligned}\quad (4.27)$$

The dynamics may then be derived exactly as in the full theory.

4.3 Results

Measurements of the chiral condensate are plotted in figure 1 for $N = 30$, $T = 50$, $dt = 10^{-4}$, $N_f = 2$, $\tilde{\mu} = \sqrt{N} \cdot \mu = 2$ and a range of masses $\tilde{m} = N \cdot m$. The blue disks in the plot represent the simulation, the blue line is the analytical result, the green squares represent the phase quenched simulation and the green line is the analytical result for the phase quenched theory. The phase quenched theory converges correctly in the full mass range, while the full theory only converges correctly for masses greater than some critical value around, $\tilde{m}_{\text{critical}} \approx 15$. Measurements of the baryon number density have been plotted in the lower panel of figure 1 for the same parameter values and same representation of lines. Again the phase quenched theory converges correctly in the full mass range, while the full theory fails to converge for masses less than $\tilde{m}_{\text{critical}}$. The convergence is admittedly not spot on for all $\tilde{m} > \tilde{m}_{\text{critical}}$ but it becomes better as \tilde{m} is raised.

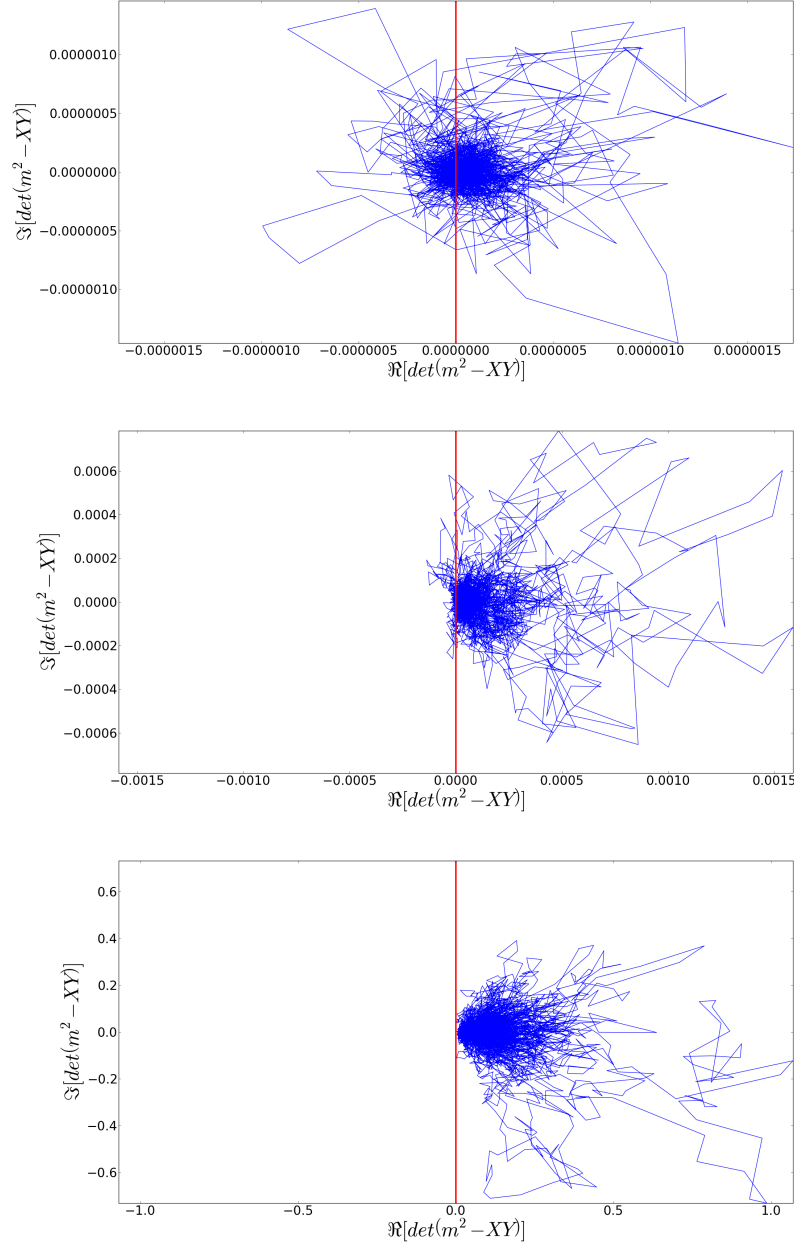


Figure 3. Flow plots of the determinant during a Langevin simulation of the chiral random matrix theory for $T = 50$, $dt = 10^{-4}$, $N = 30$, $\tilde{\mu} = 2$ and $\tilde{m} = 5, 10$, and respectively 15. Comparing to the measurement of the chiral condensate and baryon number density, we find that correct convergence, and restriction of the determinant to the right half plane, share the same domain of masses.

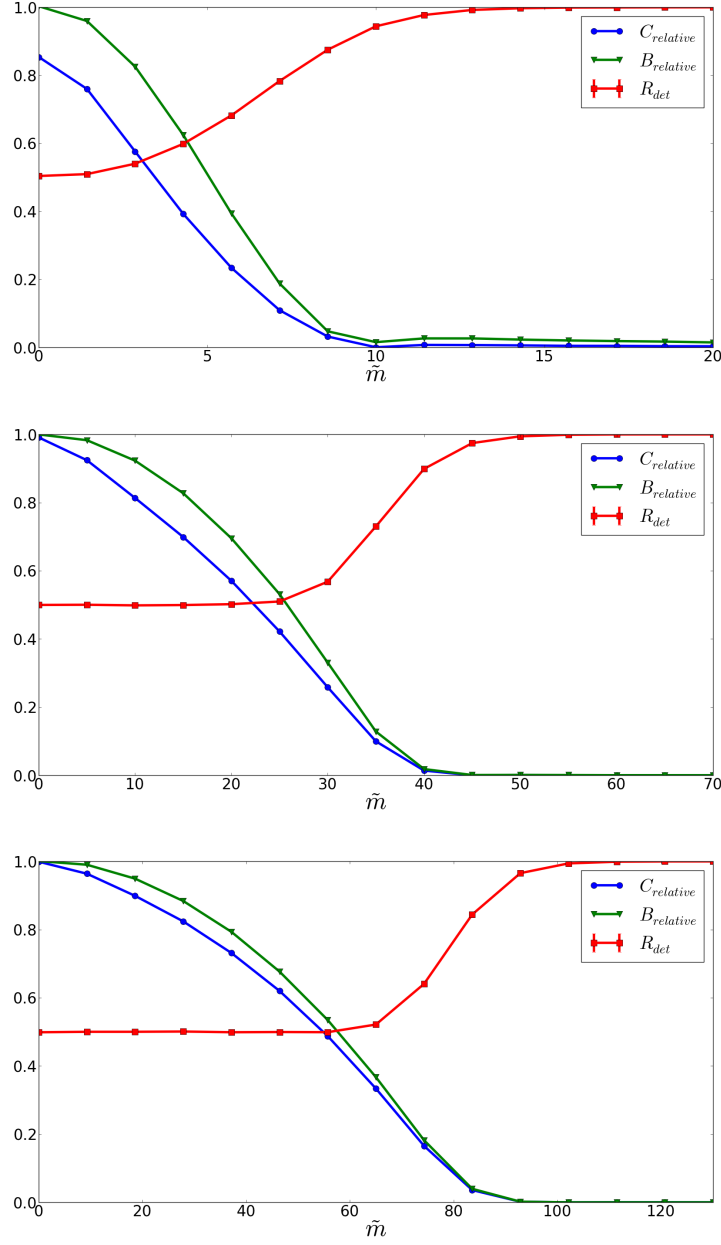


Figure 4. Comparison of the ratio of determinants in the positive half plane and convergence of the the chiral condensate and baryon number density during a Langevin simulation of the chiral random matrix theory for $N = 30$ and $\tilde{\mu} = 2, 5, 8$. We observe that failed convergence and the appearance of determinants in both half planes share the same domain of masses. As expected the range varies substantially for the three values of $\tilde{\mu}$.

Since the drift becomes singular, when the determinant is close to zero, the step size, dt , has to be chosen quite small in order to keep the finite step size effects at a minimum. In figure 2 we plot $\langle \bar{\eta}\eta \rangle_{CLD}/N$ as a function of dt for $t = 50$, $N = 30$, $N_f = 2$, $\tilde{\mu} = 2$ and $\tilde{m} = 5$. The result of the simulation is found to settle around $dt = 10^{-4}$, but not to the analytical result. Instead the dynamics fall closer to the phase quenched theory, see figure 1. We have simulated the chiral random matrix theory at various matrix sizes N and the observed behavior is independent of N . In particular, the failed convergence at small masses is present even for $N = 2$ where the singularity of the drift term is no problem to deal with numerically.

The failed convergence of the complex Langevin dynamics at small masses may be linked to the ambiguities of the drift term due to the logarithm by plotting the values of the determinant during the simulation for different values of the mass. This is done in figure 3 for $\tilde{\mu} = 2$ and $\tilde{m} = 5, 10, 15$; the cloud of determinants is found to move from the origin to the right half plane as \tilde{m} is raised to $\tilde{m}_{\text{critical}}$. This is exactly the point at which the cut of the logarithm safely may be ignored and correct convergence sets in. In order to quantify this further we plot in figure 4 the ratio of determinants in the right half plane, R_{det} , with a measure of convergence for the chiral condensate

$$C_{\text{relative}} \equiv \left| \langle \bar{\eta}\eta \rangle_{\text{CLD}} - \langle \bar{\eta}\eta \rangle_{\text{analytical}} \right| / \left| \langle \bar{\eta}\eta \rangle_{\text{analytical}} \right|, \quad (4.28)$$

and the baryon number density

$$B_{\text{relative}} \equiv \left| \langle \eta^\dagger \eta \rangle_{\text{CLD}} - \langle \eta^\dagger \eta \rangle_{\text{analytical}} \right| / \max \left| \langle \eta^\dagger \eta \rangle_{\text{CLD}} \right|, \quad (4.29)$$

against \tilde{m} for three different values of $\tilde{\mu}$. The value of $\tilde{m}_{\text{critical}}$ changes as $\tilde{\mu}$ is raised, but the region of failed convergence corresponds to the presence of determinants in the left half plane in all three cases.

The complex Langevin simulation of chiral random matrix theory suggests a general criterion for actions containing a logarithm of a determinant, which must be satisfied in order for complex Langevin dynamics (using the standard derivative of the logarithm) to yield correct convergence: *measurements can only be trusted if the flow of the determinant does not frequently trace out a path surrounding the origin.*

5 Two $U(1)$ models

We shall now use the above criterion to understand the regions of successful and failed convergence in two previously studied $U(1)$ models [11, 18]. The action in the first

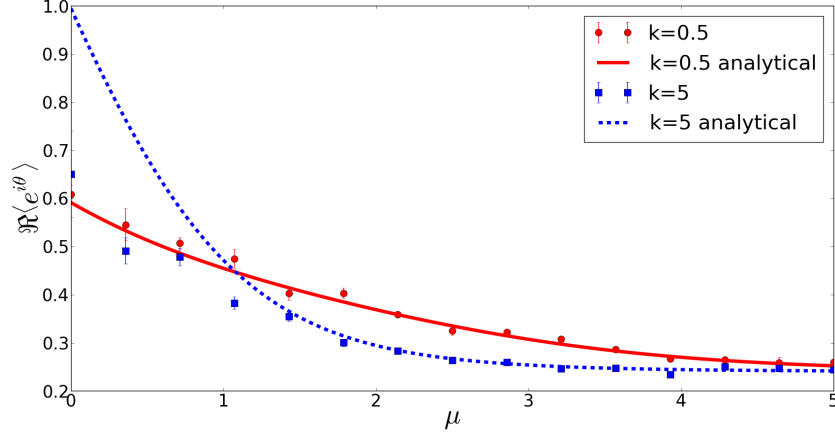


Figure 5. Measurements of $\langle e^{i\theta} \rangle$ for $T = 100$, $dt = 10^{-4}$, $\beta = 1$, $\mu \in [0, 5]$ and the two values $\kappa = 0.5$ and $\kappa = 5$. For the first value of κ correct convergence is found in the full μ range, while failed convergence is found for $\mu \gtrsim 1.5$ for the second value of κ .

model is

$$S = -\beta \cos \theta - \log(1 + \kappa \cos(\theta - i\mu)), \quad (5.1)$$

and leads to the drift term (again ignoring the cut)

$$-\frac{\partial S(\theta)}{\partial \theta} = -\beta \sin \theta - \frac{\kappa \sin(\theta - i\mu)}{1 + \kappa \cos(\theta - i\mu)}. \quad (5.2)$$

In [18] successful convergence of complex Langevin with the above drift term was found for values of κ between 0 and 1. In figure 5 we show plots of $\Re\langle e^{i\theta} \rangle$ with $\kappa = 0.5$ and $\kappa = 5$. As in [18] we find perfect convergence for complex Langevin for κ between 0 and 1 but for $\kappa = 5$ we find failed convergence when the standard derivative of the logarithm is used. The correct and failed convergence may be predicted by studying the dynamics of the argument of the logarithm. As an example we plot in figure 6 two paths which M traces out for $\mu = 0.5$: With $\kappa = 0.5$ the cut can safely be ignored, while for $\kappa = 5$, where the convergence fails, the trajectory circles the origin.

The second $U(1)$ model we consider, illustrates that an oscillating phase of the argument of the logarithm, when sampling the original real valued manifold of the integral, does not necessarily imply an oscillating phase, when sampling in the complexified space of the Langevin simulation. This example is found in the eigenvalue representation of one dimensional QCD first studied with complex Langevin in [11].

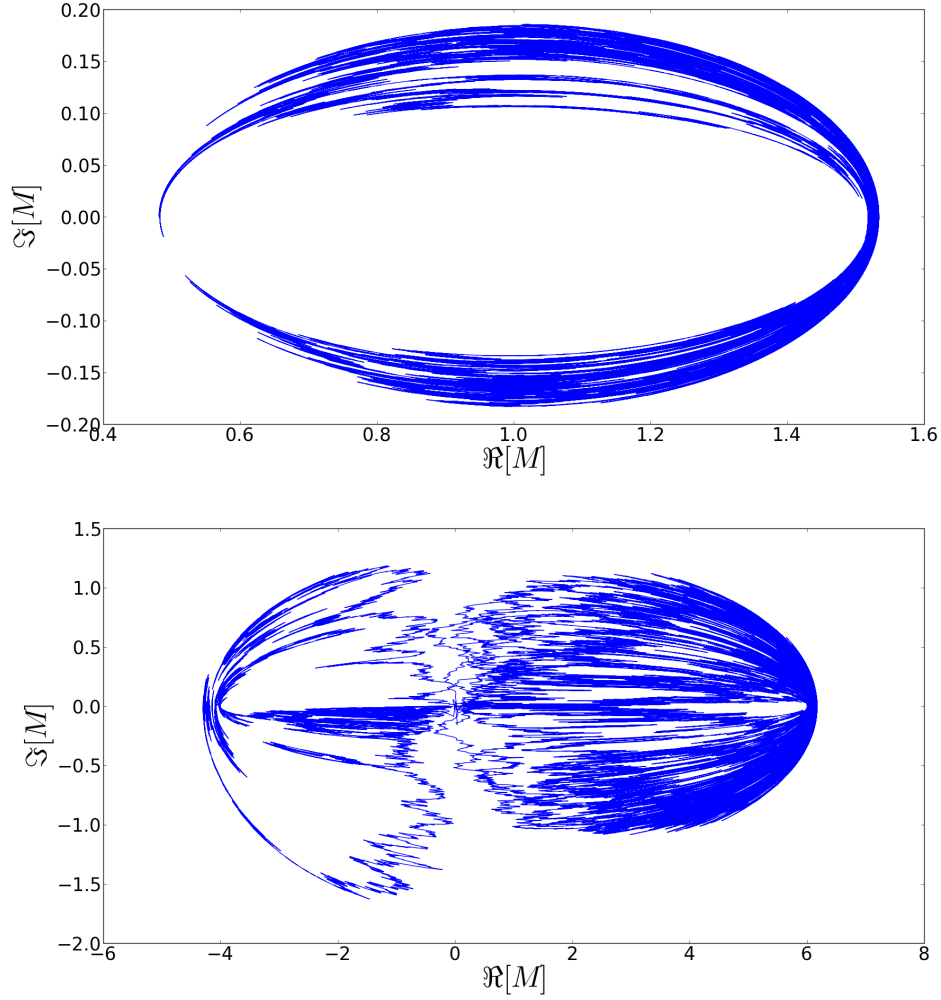


Figure 6. Flow of the argument of the logarithm, $M \equiv 1 + \kappa \cos(\theta - i\mu)$, for the U(1) link model in (5.1) with $\mu = 0.5$. Successful convergence is found for the path in the top figure with $\kappa = 0.5$, where the cut safely may be ignored, while incorrect convergence is found for the path in the lower plot generated at $\kappa = 5$. (Note that the ranges on the axis in the two plots are different.)

The partition function is given by

$$Z = \int_{-\pi}^{\pi} \frac{d\alpha}{2\pi} e^{\log(M(\alpha))}, \quad (5.3)$$

with the argument of the logarithm given by

$$M(\alpha) = 1 - \frac{\cosh[n(\mu + i\alpha)]}{\cosh(n\mu_c)}. \quad (5.4)$$

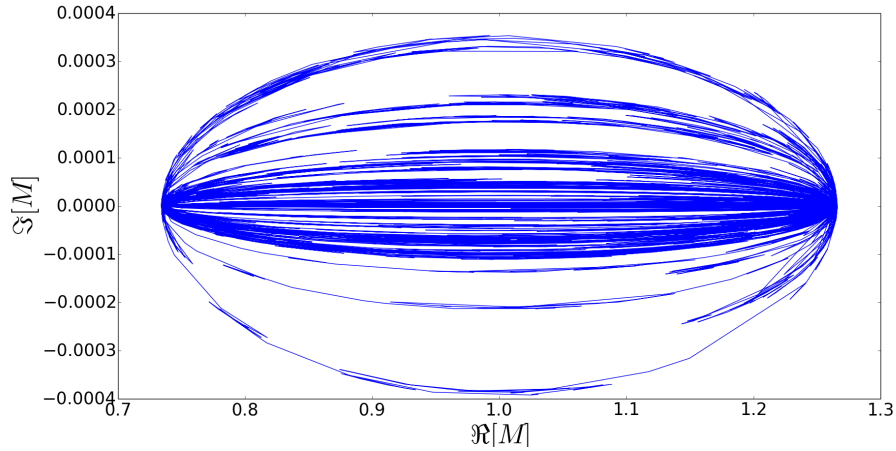


Figure 7. The trajectory which the argument of the logarithm in the action of a one dimensional QCD eigenvalue integral, Eq. (5.4), traces out during the complex Langevin simulation. The parameters used here are $\mu = 1$, $\mu_c = 0.4$, $n = 4$ which correspond to the region with a strong sign problem in the original integral. The flow does not circle the origin and the complex Langevin simulation converges nicely.

As demonstrated in [11] complex Langevin successfully computes the average of the chiral condensate

$$\Sigma(\alpha) = \frac{1}{\sinh(\mu + i\alpha) + \sinh(\mu)} \quad (5.5)$$

even for large values of n and $\mu > \mu_c$ where M oscillates wildly in the original real valued integral. At first this may appear to be in contrast to what we have observed in chiral random matrix theory. In particular, since the oscillations are essential in order to obtain the correct chiral condensate [41] when working with a real valued angle α . However, as shown in figure 7 the path which $M(\alpha)$ traces out during the complex Langevin simulation, surrounds $M = 1$ and does not enter the negative half plane. Therefore successful measurements may be performed even when one ignores the ambiguities related to the logarithm.

6 Conclusions and outlook

We have performed complex Langevin simulations of a chiral random matrix theory which, in the microscopic limit, is equivalent to QCD at nonzero chemical potential. The virtue of the random matrix theory is that it allows for an exact analytic solution and hence to test if the complex Langevin dynamics converges correctly. While the

complex Langevin simulation works at larger values of the quark mass we found that it converges incorrectly for small masses. As in full QCD the sign problem in chiral random matrix theory is due to the complex valued fermion determinant. In the complex Langevin dynamics the fermion determinant enters through a logarithmic term in the action. Because the logarithm is a multivalued function it leads to an ambiguity when defining the Langevin force: should one take the derivative of the logarithm using the standard form, or should one try to incorporate the cut of the principal part of the logarithm. The standard choice used in the literature is to ignore the cut of the principal part of the logarithm and this is also the choice with which we implemented the complex Langevin dynamics for chiral random matrix theory. We have demonstrated that the failure of the complex Langevin dynamics at small values of the quark mass occurs in the region of parameters, where the fermion determinant frequently circles the origin during the complex Langevin flow. This is exactly the region where the ambiguity of the logarithm is relevant. Based hereon it is natural to propose a criterion, which must be satisfied in order to safely use the standard form of the derivative of the logarithm in complex Langevin dynamics; the determinant is not allowed frequently to trace out a path surrounding the origin. This criterion has been used to predict regions of successful and failed convergence in two previously studied $U(1)$ models.

The phase of the fermion determinant in QCD at nonzero chemical potential is known to cover the full range $[-\pi, \pi]$, when sampling on the real manifold, see eg. [39, 40]. As we have exemplified in a $U(1)$ model this behavior is not necessarily reproduced in the complexified Langevin space, so it is possible that the cut may be ignored in a simulation of QCD. This may of course be checked explicitly in any given complex Langevin simulation of full QCD by plotting the trajectory of the fermion determinant during the Langevin flow.

The success and failure, observed as a function of the quark mass in the Langevin simulation of chiral random matrix theory, is quite similar to that observed in the 0+1 dimensional Thirring model [19]. Langevin simulations of the Thirring model have not been performed as a part of this work, but it is natural to expect that the same mechanism is responsible for the incorrect dynamics observed in [19].

Other issues of complex Langevin dynamics have been solved by introduction of techniques such as the adaptive step size and gauge cooling. It is possible that the ambiguities associated with the logarithm of the fermion determinant may be avoided by altering the dynamics of the simulation. This is the challenge ahead¹.

¹Some first attempts in this direction have been presented in [42]

Acknowledgments: We wish to thank Poul Henrik Damgaard, Gert Aarts, Joyce C. Meyers, as well as participants and organizers of XQCD 2013 at the AEI in Bern for discussions. Jac Verbaarschot and Gert Aarts are thanked for insightful comments on the manuscript. The work of KS was supported by the *Sapere Aude program* of The Danish Council for Independent Research.

A $U(1)$ model with flow towards the real axis

In this appendix we revisit the model introduced in [20] as a simplification of a $U(1)$ -link model. This case is special in that the argument of the logarithm flows to the real axis rather than fluctuating in the complex plane.

Consider a single compact degree of freedom, $\theta \in [-\pi, \pi]$, and an action

$$S(\theta) = -\beta \cos \theta - \log(\cos(\theta)). \quad (\text{A.1})$$

Calculating the drift term (by ignoring the cut)

$$-\frac{\partial S(\theta)}{\partial \theta} = -\beta \sin \theta - \tan \theta \quad (\text{A.2})$$

it was found [20] that measurements of $\langle \cos \theta \rangle$ are successful for large values of β but fail for $\beta \lesssim 3.5$, see figure 8. The region of failed convergence, $\beta \lesssim 3.5$, may be predicted by plotting a measure of the simulated sign problem, $|\langle \cos \theta \rangle_{CLD}| / \langle |\cos \theta| \rangle_{CLD}$, as done in figure 9. When β is lowered to around 3.5, the argument of the logarithm, $\cos \theta$, starts changing sign, and this is also the value, below which the measurements with the complex Langevin dynamics fail.

Also shown in figure 8 is the result for $\langle \cos \theta \rangle$ computed with the phase quenched action

$$S^{\text{PQ}}(\theta) = -\beta \cos \theta - \Re[\log(\cos(\theta))]. \quad (\text{A.3})$$

As already observed in [38] we see that the measurement converges to the phase quenched results. The reason why the convergence to the phase quenched result is exact in this case can be understood from the flow diagram in figure 10. The flow is attracted to the real axis, where the logarithm takes the form

$$\log x = \Re[\log x] + i\pi \cdot \Theta(-x), \quad (\text{A.4})$$

so ignoring the discontinuity of the imaginary part, is in this case tantamount to working in the phase quenched theory. In [38] attempts to include the effect of the step function in the complex Langevin flow were discussed. These have been reexamined in [42].

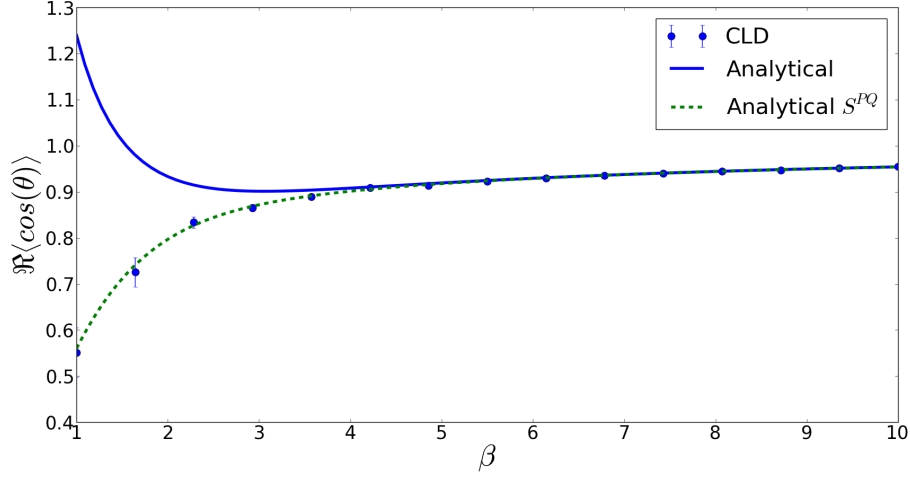


Figure 8. Langevin measurement of $\cos \theta$ for $T = 200$, $dt = 0.002$ and the drift term given in (A.2). The dynamics produces failed convergence for small β , where the results of the phase quenched theory in (A.3) are produced instead.

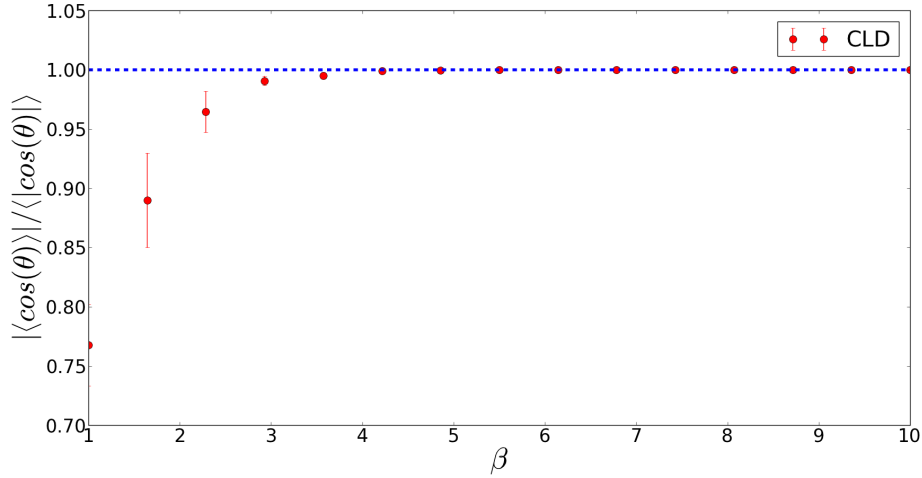


Figure 9. Plot of the simulated sign problem $|\langle \cos \theta \rangle_{CLD}| / |\langle \cos \theta \rangle_{CLD}|$ for the drift in (A.2) with $T = 200$, $dt = 0.002$ and a range of β values. We find that the sign problem region is coinciding with the region of failed convergence in figure 8.

It should be noticed that the singular behavior of the logarithm at the origin does not seem to pose a problem. One may convince oneself of this by studying the action

$$S(x) = ax^2 - \log(x^2), \quad (\text{A.5})$$

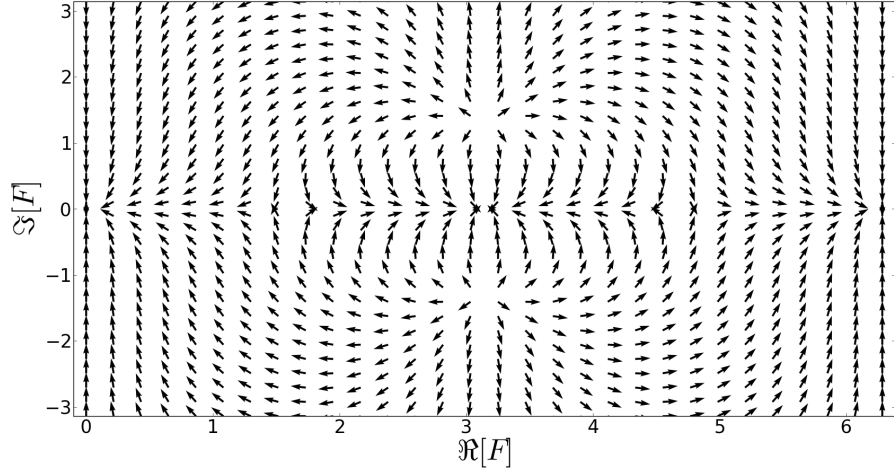


Figure 10. Flow diagram for the drift in (A.2) with $\beta = 0.5$. The trajectories are attracted to the real axis.

which forces x , and therefore also x^2 , close to the singularity for $a > 0$. Simulations works beautifully for adaptive or small step sizes, but if the argument of the logarithm is allowed to change phase as for the slightly generalized action

$$S(x) = x^2 - \log(m^2 - x^2), \quad (\text{A.6})$$

then complex Langevin dynamics (using $\partial_z \log z = 1/z$) fails.

References

- [1] G. Aarts, PoS LATTICE **2012**, 017 (2012) [arXiv:1302.3028 [hep-lat]].
- [2] P. de Forcrand, PoS LAT **2009**, 010 (2009) [arXiv:1005.0539 [hep-lat]].
- [3] K. Splittorff, PoS LAT **2006**, 023 (2006) [hep-lat/0610072].
- [4] P. H. Damgaard and H. Hufel, Phys. Rept. **152**, 227 (1987).
- [5] G. Aarts, E. Seiler and I. -O. Stamatescu, Phys. Rev. D **81**, 054508 (2010) [arXiv:0912.3360 [hep-lat]].
- [6] G. Aarts, F. A. James, E. Seiler and I. -O. Stamatescu, Eur. Phys. J. C **71**, 1756 (2011) [arXiv:1101.3270 [hep-lat]].
- [7] G. Aarts, F. A. James, E. Seiler and I. -O. Stamatescu, PoS LATTICE **2011**, 197 (2011) [arXiv:1110.5749 [hep-lat]].

- [8] G. Aarts, Phys. Rev. Lett. **102**, 131601 (2009) [arXiv:0810.2089 [hep-lat]].
- [9] G. Aarts, JHEP **0905**, 052 (2009) [arXiv:0902.4686 [hep-lat]].
- [10] G. Aarts, PoS LAT **2009**, 024 (2009) [arXiv:0910.3772 [hep-lat]].
- [11] G. Aarts and K. Splittorff, JHEP **1008**, 017 (2010) [arXiv:1006.0332 [hep-lat]].
- [12] G. Aarts, L. Bongiovanni, E. Seiler, D. Sexty and I. -O. Stamatescu, Eur. Phys. J. A **49**, 89 (2013) [arXiv:1303.6425 [hep-lat]].
- [13] E. Seiler, D. Sexty and I. -O. Stamatescu, Phys. Lett. B **723**, 213 (2013) [arXiv:1211.3709 [hep-lat]].
- [14] G. Aarts, L. Bongiovanni, E. Seiler, D. Sexty and I. -O. Stamatescu, Eur. Phys. J. A **49**, 89 (2013) [arXiv:1303.6425 [hep-lat]].
- [15] D. Sexty, arXiv:1307.7748 [hep-lat].
- [16] J. C. Osborn, Phys. Rev. Lett. **93**, 222001 (2004) [hep-th/0403131].
- [17] J. Bloch, F. Bruckmann, M. Kieburg, K. Splittorff and J. J. M. Verbaarschot, Phys. Rev. D **87**, 034510 (2013) [arXiv:1211.3990 [hep-lat]].
- [18] G. Aarts and I. -O. Stamatescu, JHEP **0809**, 018 (2008) [arXiv:0807.1597 [hep-lat]].
- [19] J. M. Pawłowski and C. Zielinski, Phys. Rev. D **87**, 094503 (2013) [arXiv:1302.1622 [hep-lat]].
- [20] J. Ambjorn, M. Flensburg and C. Peterson, Nucl. Phys. B **275**, 375 (1986).
- [21] K. Jacobs, *Stochastic Processes for Physicists*, Westview Press, 2010.
- [22] G. Parisi, Phys. Lett. B **131**, 393 (1983).
- [23] J. R. Klauder, Acta Phys. Austriaca **25**, 251 (1983).
- [24] C. Gattringer and C. B. Lang, Lect. Notes Phys. **788**, 1 (2010).
- [25] K. Splittorff and J. J. M. Verbaarschot, Phys. Rev. Lett. **98**, 031601 (2007) [hep-lat/0609076]; Phys. Rev. D **75**, 116003 (2007) [hep-lat/0702011 [HEP-LAT]]; Phys. Rev. D **77**, 014514 (2008) [arXiv:0709.2218 [hep-lat]].
- [26] J. Feinberg and A. Zee, Nucl.Phys. B504 (1997) 579.
- [27] E. V. Shuryak and J. J. M. Verbaarschot, Nucl. Phys. A **560**, 306 (1993) [hep-th/9212088].
- [28] J. J. M. Verbaarschot and I. Zahed, Phys. Rev. Lett. **70**, 3852 (1993) [hep-th/9303012].
- [29] J. J. M. Verbaarschot, Phys. Rev. Lett. **72**, 2531 (1994) [hep-th/9401059].
- [30] M. A. Stephanov, Phys. Rev. Lett. **76**, 4472 (1996) [hep-lat/9604003].
- [31] J. C. Osborn, K. Splittorff and J. J. M. Verbaarschot, Phys. Rev. Lett. **94**, 202001 (2005) [hep-th/0501210]; Phys. Rev. D **78**, 065029 (2008) [arXiv:0805.1303 [hep-th]].

- [32] T. Banks and A. Casher, Nucl. Phys. B **169**, 103 (1980).
- [33] K. Splittorff and J. J. M. Verbaarschot, Nucl. Phys. B **757**, 259 (2006) [hep-th/0605143].
- [34] J. J. M. Verbaarschot and T. Wettig, Ann. Rev. Nucl. Part. Sci. **50**, 343 (2000) [hep-ph/0003017].
- [35] G. Akemann, J. C. Osborn, K. Splittorff and J. J. M. Verbaarschot, Nucl. Phys. B **712**, 287 (2005) [hep-th/0411030].
- [36] F. Basile and G. Akemann, JHEP **0712**, 043 (2007) [arXiv:0710.0376 [hep-th]].
- [37] G. Akemann, Int. J. Mod. Phys. A **22**, 1077 (2007) [hep-th/0701175].
- [38] K. Fujimura, K. Okano, L. Schulke, K. Yamagishi and B. Zheng, Nucl. Phys. B **424**, 675 (1994) [hep-th/9311174].
- [39] M. P. Lombardo, K. Splittorff and J. J. M. Verbaarschot, Phys. Rev. D **80**, 054509 (2009) [arXiv:0904.2122 [hep-lat]].
- [40] J. Greensite, J. C. Myers and K. Splittorff, Phys. Rev. D **88**, 031502 (2013) [arXiv:1306.3085 [hep-lat]]; arXiv:1308.6712 [hep-lat].
- [41] L. Ravagli and J. J. M. Verbaarschot, Phys. Rev. D **76**, 054506 (2007) [arXiv:0704.1111 [hep-th]].
- [42] A. Møllgaard, Master Thesis, The Niels Bohr Institute, University of Copenhagen (2013).